International Journal of Energetica (IJECA)
https://www.ijeca.info
ISSN: 2543-3717 Volume 10. Issue 2. 2020 *Page 49-64*

Simulation Study of a Hybrid MPPT Controller with Enhanced Walrus Optimization and Levenberg-Marquardt Training

Daniel Kwegyir[1*], Isaac Asare[2], Felix Kwasi Inkoom[3], Derrick Darko[3], Mujeeb Iddrisu[3], Ernest Amoah[3], Priscilla Oyeladun Ajiboye[4], Peter Asigri[4], Daniel Opoku[4], Francis Boafo Effah[4]

[1234]*Kwame Nkrumah University of Science and Technology, Kumasi, GHANA*
[4]*Akenten Appiah-Menka University of Skills Training and Entrepreneurial Development, Kumasi, GHANA*

**Corresponding Author Email: daniel.kwegyir@knust.edu.gh*

Abstract –*The increasing deployment of photovoltaic (PV) systems demands efficient maximum power point tracking (MPPT) methods to optimize energy extraction under varying environmental conditions. Conventional MPPT algorithms often suffer from slow convergence and instability under fluctuating irradiance and temperature. Here we propose a hybrid MPPT controller combining an enhanced Walrus Optimization algorithm with Vigilante Selection and Juvenile Update (WOVE-NSJ) and Levenberg-Marquardt (LM) training of a feedforward neural network (FNN). This approach improves global search and local fine-tuning, achieving near-ideal tracking efficiencies of 99.98%, reduced average tracking time (0.0914 s), and minimal overshoot with near-instantaneous settling times. Benchmarking against state-of-the-art ANN-based controllers demonstrates superior transient stability and robustness. These findings suggest that the proposed WOVE-NSJ-LM-FNN controller offers a promising solution for real-time, high-performance MPPT in PV systems, enhancing power output and system reliability under dynamic conditions.*

Keywords*: Walrus Optimization, Levenberg-Marquardt Algorithm, Maximum Power Point Tracking, Feedforward Neural Networks, Photovoltaic Systems.*

Received: 09/08/2025 – Revised: 12/11/2025 – Accepted: 27/11/2025

I. Introduction

The accelerating global demand for sustainable energy solutions is driven by the urgent need to mitigate the climate crisis [1]. This transition is critical not only for reducing dependence on fossil fuels but also for securing wider societal benefits, including improved public health, enhanced energy security, and long-term economic stability [2]. Photovoltaic (PV) systems have become a dominant renewable energy technology due to their scalability, minimal environmental footprint, and relatively low maintenance requirements [3]. Global PV capacity now exceeds 1.6 TW [4], underscoring the need for continuous technological and algorithmic innovation to maximize energy yield. Despite their rapid deployment, PV modules remain inherently constrained by low conversion efficiencies [5]. This limitation makes continuous operational optimization essential to ensure maximum energy extraction. At the core of this challenge lies Maximum Power Point Tracking (MPPT), which identifies and sustains the operating point of highest power output under dynamically varying solar irradiance and temperature conditions [6].

Conventional MPPT techniques, such as Perturb and Observe (P&O) and Incremental Conductance (INC), as well as fractional-based methods, have been widely used as MPPT algorithms due to their simplicity and low computational cost [8]. However, they suffer from drawbacks, including steady-state oscillations, periodic power interruptions, and reduced reliability under rapidly changing environmental conditions [9-10]. These limitations have motivated the development of advanced

MPPT methods that incorporate intelligent control and metaheuristic optimization. Again, Artificial Neural Networks (ANNs), adaptive fuzzy controllers [11], and hybridized methods with optimization algorithms have demonstrated superior tracking accuracy and adaptability, particularly under partial shading. However, proposed hybrid methods in the literature often require extensive training datasets and introduce significant computational complexity, limiting their feasibility in resource-constrained PV systems [12].

Additionally, despite significant progress in the development of metaheuristic algorithms (MHAs) [13], the continuous demand for improved solutions to increasingly complex problems drives the need for ongoing research. This necessitates the enhancement of the accuracy of existing MHAs for MPPT applications. Such enhancements are crucial because many algorithms are based on approximations of natural behaviour and are prone to becoming trapped in local optima rather than finding a global solution. To address the limitations of existing MPPT strategies and MHAs, this work proposes a novel hybrid controller with an enhanced Walrus Optimization with Vigilante Selection and Juvenile Update Levenberg Marquardt Feedforward Neural Network (WOVE-NSJ–LM-FNN) for an MPPT controller. The controller combines the global search capabilities of an enhanced Walrus Optimization (WO) algorithm with the rapid convergence of the Levenberg-Marquardt (LM) training method.

The Walrus Optimization (WO) [14] algorithm is a recently proposed metaheuristic algorithm that has demonstrated significant versatility and effectiveness across a diverse range of complex engineering problems in the literature. The standard WO algorithm exhibits critical limitations, particularly in addressing complex, high-dimensional optimization problems. These challenges primarily stem from premature convergence and an imbalanced approach to exploration and exploitation. The random selection of vigilantes in the original WO can lead to suboptimal guidance for the population, as these experienced individuals may not always represent the most promising solutions, thus causing the algorithm to converge prematurely, especially in multimodal functions with numerous local minima. Furthermore, while juveniles are intended to introduce diversity through exploratory movements, their random and undirected exploration in the search space can result in inefficient traversal of low-quality regions, slowing convergence. This lack of a mechanism to guide juveniles towards areas of higher fitness potential or away from detrimental areas leads to suboptimal exploration, as juveniles might repeatedly explore unpromising regions.

To address these issues, we propose two primary modifications to the WO algorithm: (1) a fittest-based vigilante selection strategy and (2) a juvenile update mechanism that directs juveniles toward the safest and fittest solutions. These modifications form the basis of our new algorithm, the Walrus Optimization with Vigilante Selection and Juvenile Update (WOVE-NSJ), which enhances convergence rates, improves the balance between exploration and exploitation, and yields higher-quality solutions for complex optimization problems.

In this work, we proposed a novel hybrid MPPT controller, the WOVE-NSJ–LM-FNN MPPT, with improved accuracy and low computational requirements for solar power extraction. The key contributions made by authors are summarized below.

a) We proposed a novel hybrid MPPT controller that combines an improved Walrus Optimization algorithm with Levenberg-Marquardt Feedforward Neural Network training, yielding a hybrid MPPT controller that ensures high accuracy with reduced computational overhead and simplified tuning for real-time PV systems.
b) Again, we proposed an enhanced Walrus Optimization algorithm named WOVE-NSJ, which introduces a fittest-based vigilante selection concept and juvenile update mechanisms to improve the WO algorithm's exploration and exploitation balance.The modifications introduced improved convergence, with superior performance.

The remainder of this article is organized as follows. Section II describes the proposed photovoltaic system configuration and details the modelling of its key components, including the PV module, boost converter, and artificial neural network structure. The section further explains the modifications introduced in the Walrus Optimization algorithm and the integration of the Levenberg–Marquardt training method. Section III presents the simulation environment, dataset creation, ANN model development, performance evaluation metrics, and benchmarking procedures. Section IV discusses the results obtained, with emphasis on output power, tracking efficiency, convergence speed, and transient stability in comparison with existing controllers. Finally, Section V concludes the paper by summarizing the main contributions and highlighting possible directions for future research.

II. Proposed PV System Configuration with Hybrid MPPT Algorithm

The proposed photovoltaic system designed for this study is shown in Figure 1. The system consists of a PV module, a DC/DC boost converter controlled by the proposed ANN-based MPPT controller, and a resistive load. This system is controlled by an intelligent MPPT controller based on a hybrid training approach using a modified Walrus Optimization Algorithm (WOVE-NSJ) and the Levenberg-Marquardt (LM) algorithm for training an Artificial Neural Network (ANN). The goal of the MPPT controller is to continuously adjust the converter's duty cycle to extract the maximum possible power from the PV module under varying environmental conditions. The Maximum Power Point (MPP) on the PV (I-V) curve is where the product of voltage and current is highest, representing the peak power output. In PV systems, the MPP depends on factors like solar irradiance and cell temperature. Changes in temperature mainly affect the PV output voltage, while changes in irradiance affect the output current. To ensure a PV system operates at its maximum power output, it needs to adjust to varying environmental conditions. This is managed by a DC/DC converter controlled by an MPPT algorithm. The MPPT algorithm adjusts the converter's duty cycle to keep the system at the MPP. In the proposed design, an optimized ANN algorithm determines the optimal duty cycle by analyzing real-time solar irradiance (G) and temperature (T) data. It then adjusts the converter's operation to ensure the PV system operates at its maximum power point. This adaptive approach enhances energy conversion efficiency, helping the PV system better utilize solar resources.

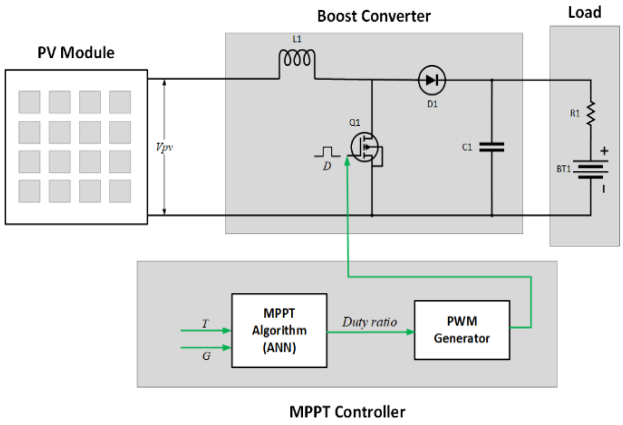

Figure 1. Proposed photovoltaic (PV) system with hybrid MPP tracker (Screenshot from MATLAB Simulink)

2.1. Proposed Modified Walrus Optimization

The Walrus Optimization (WO) is a novel addition to metaheuristic optimization algorithms, inspired by unique walrus social and behavioural patterns. Despite its novelty and performance, the WO algorithm faces several critical limitations that affect its effectiveness in solving complex, high-dimensional optimization problems. These challenges include premature convergence and an imbalanced approach to exploration and exploitation, which we will elaborate on below. In the standard WO, the random selection of vigilantes significantly influences the algorithm's convergence. Vigilantes, who guide the migration phase, are chosen at random. This can result in suboptimal guidance for the population since vigilantes represent experienced individuals within the algorithm. Random selection does not ensure that the most promising solutions will guide the rest of the population. Consequently, this can lead to the walruses following less fit individuals, causing premature convergence, particularly when dealing with multimodal functions with numerous local minima. Moreover, the balance between exploration and exploitation is essential in any optimization algorithm. In WO, juveniles (young walruses) play a crucial role in introducing diversity through exploratory movements. However, their movements are not directed toward known high-quality solutions; instead, they randomly explore the search space. This approach can result in excessive exploration in low-quality regions, thereby reducing the algorithm's efficiency and slowing convergence toward optimal solutions. Additionally, the WO algorithm lacks a mechanism to guide juveniles toward areas with higher fitness potential or away from harmful areas within the search space. In the original WO, juveniles perform independent, random movements without the influence of high-fitness solutions. This can lead to suboptimal exploration, as juveniles may repeatedly explore regions far from optimal solutions or in dangerous areas. This behaviour limits the algorithm's ability to refine the search efficiently and produces solutions of poor quality. To address these issues, we propose two primary modifications: (1) a fittest-based vigilante selection strategy and (2) a juvenile update mechanism that directs juveniles toward the safest and fittest solutions. These modifications result in the Walrus Optimization with Vigilante Selection and Juvenile Update (WOVE-NSJ) algorithm, which is designed to enhance convergence rates, improve the balance between exploration and exploitation, and yield higher-quality solutions for complex optimization problems.

2.2. New Vigilante Selection Strategy

In the original WO, vigilantes are selected randomly, which can hinder convergence by not using the highest-quality solutions as guides. We propose using the two fittest male walruses in the population as vigilantes, thereby ensuring that only high-quality solutions influence the migration phase. Let $X_{male,i}$ represent the position of each male walrus, and f(X) represent the fitness function of the male walrus i. The new vigilantes are defined in (1) and (2).

$$X_{V1} = X_{male,1} \quad (1)$$

$$X_{V2} = X_{male,2} \quad (2)$$

In (1) and (2), $X_{male,1}$ and $X_{male,2}$ are the positions of the top two fittest male walruses, respectively. The updated equation for the walrus position based on the new selection of vigilantes is given in (3).

$$X_{i,j}{}^{t+1} = X_{i,j}^{t} + (X_{V1} - X_{V2}).\beta_i.r_3^2 \quad (3)$$

In (3), X_{V1} and X_{V2} are the positions of the two fittest male walruses as selected, and β_i is the adaptive migration step factor for walrus i. This new selection strategy uses the most successful individuals (fittest males) to influence the population's migration to improve convergence rates and enhance exploration.

2.3. Enhanced Juvenile Update Strategy

In this paper, we modify the juvenile update equation to enable them to move closer to the fittest and safest solution in the search space. The new position update is based on two primary factors: closeness to the fittest solution (i.e., best solution found so far) and safest position within the search space (taken as an averaged position between the fittest solution and the second well-performing individual calculated with (4).

$$X_{safe,j} = \frac{X_{best,j} + X_{best-second,j}}{2} \quad (4)$$

In (4), X_{safe} is the safest position in the j^{th} dimension in the search space, and $X_{best-second}$ is the second-best position in the j^{th} dimension in the search space.

The juvenile's position is updated by moving it towards a position between the best solution and safest position with a random weighting to retain exploration. We express the update equation for the i^{th} juvenile in the j^{th} dimension by (5).

$$X_{juv,i,j}^{i+1} = X_{juv,i,j} + r.\left(X_{Best;j} - X_{juv,i,j}\right) + (1 - r).\left(X_{safe,j} - X_{juv,i,j}\right) \quad (5)$$

In (5), $X_{juv,i,j}^{i+1}$ is the updated position of the i^{th} juvenile in the j^{th} dimension, $X_{Best;j}$ is the position of the best walrus in the j^{th}, $X_{safe,j}$ is the safest position in the j^{th} dimension, and r is a random number between 0 and 1, which allows the juvenile to move in a balanced direction between the fittest and safest solutions. The pseudo code for implementing the proposed WOVE-NSJ is given in Table 1a.

Table 1a. Pseudo code

Start	***Simulation of Walrus Optimization Algorithm***
1	***Input:*** *Set parameters of WO i.e., population size, iteration number, proportion of males and females.*
2	*Generate initial positions of walruses based on problem parameters i.e., dimension*
3	*Calculate the initial fitness of walruses based on the initial positions in the search space.*
4	***While*** *iter < maximum iteration*
5	***If*** *current walrus is the fittest found so far:*
6	*Update second best position and its fitness to the previous best values*
7	*Update best position and best score to the current walrus*
8	***Else if*** *the current walrus is the second fittest:*
9	*Update second best position and its fitness accordingly*
10	*Calculate the safest position based on (4)*
11	*Calculate danger and safety signals*
12	***If*** $\lvert danger\ signal \rvert \geq 1$ *// begin exploration*
13	*Sort all male walruses in ascending order and select the fittest amongst them*
14	*Update positions of walruses using (3)*
15	***Else:*** *// begin exploitation*
16	***If*** *safety signal ≥ 0.5: // breeding behaviour*
17	***For*** *each male walrus:*
18	*Update position of walruses using Halton sequence*
19	***For*** *each female walrus:*
20	*Update position by moving them towards the fittest males*
21	***For*** *each juvenile:*
22	*Update position by moving them towards best and safest position using (5)*
23	***Else if*** $\lvert danger\ signal \rvert \geq 0.5$: *// initiate gathering of walrus*
24	*Update position of each walrus using gathering mechanism*
25	***Else:*** *// initiate fleeing of walruses*
26	*Update position of each walrus using fleeing mechanism*
27	*Update positions of all walruses and apply boundary conditions*
28	*Increment iter and store best score and best position*
End	***Simulation***

2.4. Levenberg-Marquardt Training Algorithm

The Levenberg-Marquardt (LM) algorithm is used as a second-stage training algorithm in the proposed hybrid training approach to refine the artificial neural network parameters for Maximum Power Point Tracking (MPPT). The LM training algorithm is a highly efficient curve-fitting method suitable for small to medium-sized networks where high precision and fast convergence are critical. It is also particularly useful for regression problems such as predicting the optimal duty cycle for a boost converter, as it combines the advantages of both Gauss-Newton and gradient descent algorithms. It also converges rapidly near the error surface minimum. It is based on these reasons that the authors selected the LM in the hybrid approach. After the initial weights and biases of the ANN are optimized and selected using the modified Walrus Optimization Algorithm (WOVE-NSJ), the LM algorithm performs supervised fine-tuning to minimize the network's output error. The proposed hybrid training approach uses the improved global search capabilities of WOVE-NSJ and the fast local convergence properties to ensure good accuracy of the tracking model.

2.5. Proposed Artificial Neural Network Hybrid Training Workflow

To enhance the accuracy, robustness, and convergence speed of the Maximum Power Point Tracking (MPPT) controller, a hybrid training workflow is developed for the Artificial Neural Network (ANN). The workflow combines the global search capabilities of the Improved Walrus Optimization Algorithm (WOVE-NSJ) with the local refinement strengths of the Levenberg-Marquardt (LM) training algorithm. Figure 2 illustrates the sequential training process involved in the proposed hybrid system. Figure was conceptualised and developed by authors using Microsoft Visio Software Version 2021).

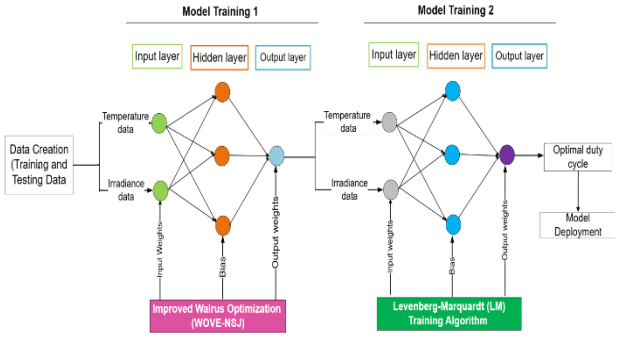

Figure 2. Proposed Hybrid System – Workflow of WOVE-NSJ-based initialization followed by LM-based fine-tuning for ANN training

The workflow consists of two main phases: global weight initialization using the WOVE-NSJ algorithm and local fine-tuning using the Levenberg–Marquardt (LM) algorithm. In the global phase, a dataset of irradiance and temperature values with corresponding optimal duty cycles is generated from PV system simulations employing a Perturb and Observe (P&O) MPPT controller. This dataset is divided into training and testing sets and used to train the ANN, where WOVE-NSJ performs global optimization of input weights, biases, and output weights by minimizing the mean squared error (MSE) between the predicted and target duty cycles. In the local fine-tuning phase, the WOVE-NSJ-optimized parameters are used as initial values for the LM algorithm, which further refines the network parameters using the same training data to achieve faster convergence and improved accuracy. The final optimized FNN is then implemented in a Simulink-based MPPT controller, where it processes real-time simulated irradiance and temperature inputs to compute the optimal duty cycle for regulating the DC/DC boost converter and ensuring continuous maximum power extraction. A summary of the training process is illustrated in Figure 3.

Figure 3. Proposed hybrid training algorithm

III. Simulation Setup and Parameter Setting

This section outlines the simulation environment, component parameters, data creation, and testing scenarios used to evaluate the performance of the proposed WOVE-NSJ-LM ANN-based MPPT controller. The goal was to test the controller under realistic environmental variations and benchmark its performance against alternative ANN-based MPPT controllers.

3.1. Simulation Environment

The parameters of the simulation environment are provided in Table 1.

Table 1. Parameters of Simulation Environment

Parameter	Description
Software	MATLAB R2022b with Simulink and Neural Network Toolbox
Hardware	Intel Core i7, 20 GB RAM
Solver Type	Fixed-step, Discrete

3.2. Training, Testing and Validation Dataset Creation

To generate the dataset for training and testing the Artificial Neural Network (ANN), a conventional MPPT technique, the Perturb and Observe (P&O) method, was modelled in MATLAB/Simulink as a controller for a PV system. The simulation of the PV system with a P&O is shown in Figure 4. The parameters of the PV model and boost converter used for the Simulink model are given in Table 2 and Table 3 respectively.

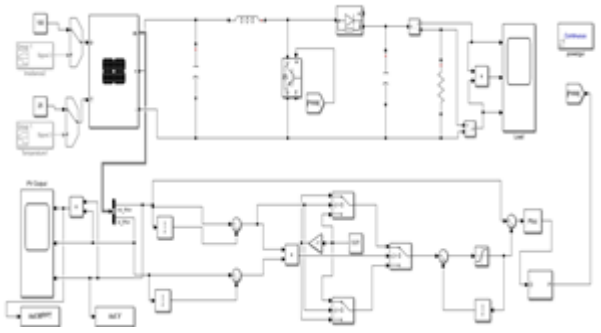

Figure 4. Simulation of a PV system with P&O as MPPT controller (Screenshot from MATLAB Simulink)

Table 2. Simulation Parameters of PV Module

Parameter	Value
Open circuit voltage (V_{oc})	329.0 V
Short circuit current (I_{sc})	24.63 A
Maximum power voltage (V_{mp})	263.0 V
Maximum power current (I_{mp})	22.83 A
Maximum power (P_{max})	6004.29 W

Table 3. Parameters of DC-DC Boost Converter

Parameter	Value
Input capacitor	5000 µF
Inductor	2.5 mH
Output capacitor	250 µF
Switching frequency	25 kHz
Load resistance	200 Ω

The baseline P&O controller was subjected to a wide range of irradiance and temperature values to simulate realistic PV operating conditions. Irradiance was varied from 100 W/m² to 1000 W/m² in steps of 10 W/m². For each irradiance level, temperatures between 18°C and 38°C were applied. Each simulation was run for 0.6 seconds with a sampling time of 1e-4 seconds to ensure that the PV system dynamics reached steady state. Although each simulation produced 6000 samples, only the final steady-state values of the RMS PV output voltage and boost converter output voltage were recorded. These values were then used to compute the corresponding duty cycle ratio for each irradiance and temperature combination. In total, 1,911 unique duty cycle data points were obtained from all simulations. The dataset was divided into training, testing, and validation subsets to ensure effective learning and generalization of the ANN. This data creation approach ensured that the ANN training dataset captured the essential nonlinear relationships between irradiance, temperature, and duty cycle and avoided redundancy from transient simulation data.

3.3. ANN Model Development

The Artificial Neural Network (ANN) model was developed in MATLAB to predict the duty cycle of the boost converter based on irradiance and temperature inputs. The model was designed and trained using a hybrid approach described earlier that integrates the Modified Walrus Optimization Algorithm for weight initialization and the Levenberg-Marquardt algorithm for fine-tuning. The ANN model building and training with the WOVE-NSJ and benchmarking with other selected algorithms were done with a MATLAB script. The dataset generated from PV system simulations was imported into MATLAB. Each data record consisted of solar irradiance, cell temperature, and corresponding duty cycle. The dataset was normalized and divided into training (70%), validation (15%), and testing (15%) subsets to ensure effective generalization of the ANN. The ANN was structured as a feedforward neural network with two input neurons, i.e., irradiance and temperature, ten hidden neurons with a sigmoid (logsig) activation function, and one neuron with a linear

(purelin) activation function for duty cycle prediction. The WOVE-NSJ algorithm was applied to optimize the initial weights and biases of the ANN. The optimization was formulated as a minimization problem, with the normalized mean squared error (NMSE) between the predicted and actual duty cycle serving as the objective function. After WOVE-NSJ had produced the optimal weights, the ANN was retrained using the Levenberg-Marquardt (LM) algorithm. The trained ANN was exported to Simulink using the gensim function in MATLAB as an MPPT controller within the PV system simulation framework. The PV system with the WOVE-NSJ-FNN controller is given in Figure 6. The parameters used in the model creation for all algorithms are given in Table 4. The training MSEs of all algorithms are compared in Figure 5.

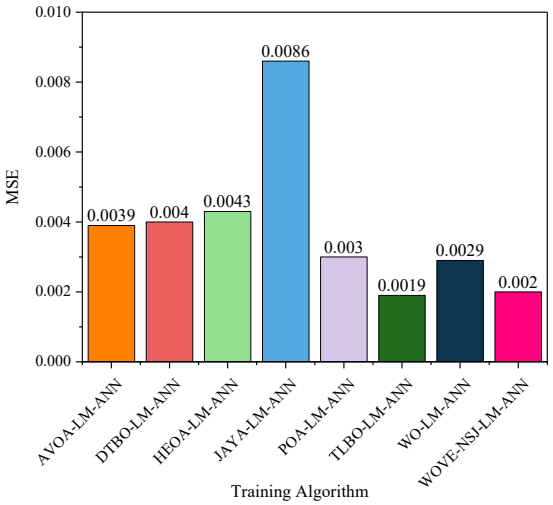

Figure 5. Training MSEs of Algorithms

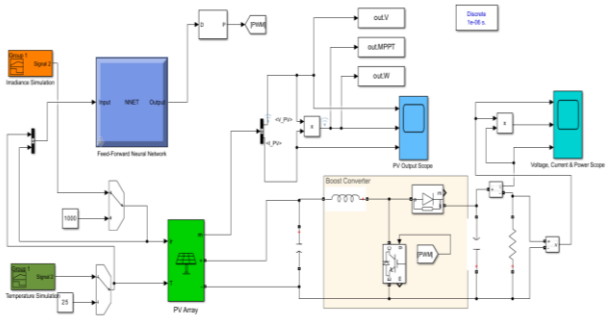

Figure 6. Simulink model of PV system with FNN controller (Screenshot from MATLAB Simulink)

Table 4. Parameters for ANN Model Building

Parameter	Specification
Input Variables	Solar irradiance, Cell temperature
Output Variable	Duty cycle of boost converter
Network Type	Feedforward Neural Network (FFNN)
Hidden Layer Neurons	10
Activation Function	Sigmoid (logsig)
Training Algorithm (Stage 1)	WOVE-NSJ and all selected benchmarking algorithms
Training Algorithm (Stage 2)	Levenberg-Marquardt (LM) fine-tuning
Training Epochs (LM)	1000 (maximum)
Performance Goal	1×10^5
Minimum Gradient	1×10^7
Data Division	70% Training, 15% Validation, 15% Testing
Export Method	gensim (for Simulink integration)
Population size	50 for all algorithms in model training 1
Maximum iterations	1000 for all algorithms in model training 1
Search space bounds	[−1, +1][-1,+1]

3.4. Performance Evaluation Metrics

We assessed the performance of the proposed WOVE-NSJ-LM-trained Artificial Neural Network (ANN) MPPT controller and compared it with other benchmark methods, using a set of quantitative metrics. The metrics capture key aspects of the controller, such as energy efficiency, controller responsiveness, and control stability. The specific metrics used are discussed below.

Output Power

This metric quantifies the electrical power extracted from the PV system at steady state. It is a direct indicator of the controller's effectiveness in tracking the Maximum Power Point (MPP). Higher output power indicates better MPPT tracking. Power is calculated as the product of PV module voltage and current over time. The maximum and average power values are recorded for each scenario.

Tracking Efficiency

The efficiency measures how closely the power extracted by the controller approaches the theoretical maximum power of the PV module under given irradiance and temperature, calculated with (6).

$$\text{Efficiency} = \left(\frac{P_{extracted}}{P_{rated}}\right) \times 100\% \qquad (6)$$

The Efficiency is computed for each test case using predefined ideal power values at 20°C, 25°C, and 30°C.

Tracking Time

The tracking time measures how quickly the MPPT controller can converge to the maximum power point after a change in environmental conditions. In this work, we record the time duration from the beginning of a simulation scenario (or after a step change) to the point

where the output power reaches and stabilizes around the MPP.

Transient Power and Voltage Response

This captures how smoothly the controller reacts to changes in irradiance and temperature. In this work, we capture the overshoot and settling time in the power and voltage signals through dynamic simulations under changes in irradiance and temperature at predefined time intervals.

3.5. Benchmarking of Proposed Method

To evaluate the effectiveness and superiority of the proposed hybrid WOVE-NSJ-LM training method for the ANN-based MPPT controller, this study performs a comprehensive comparative analysis against seven alternative optimization algorithms in the literature. The selected algorithms are Classical Walrus Optimization (WO), Teaching-Learning-Based Optimization (TLBO), JAYA Algorithm, Hybrid Evolutionary and Arithmetic Optimizer (HEAO), Pelican Optimization Algorithm (POA), African Vulture Optimization Algorithm (AVOA), and Driving Training-Based Optimization (DTBO). Each algorithm is employed to train an ANN model in Model Training 1 using the same input-output configuration, followed by Levenberg-Marquardt training in Model Training 2. All models are subjected to identical simulation conditions for a fair and consistent performance evaluation.

IV. Results and Discussions

In this section, we discuss the performance of the proposed WOVE-NSJ-LM MPPT controller compared to the benchmarking controllers stated earlier in subsection 4.5, under varying irradiance and temperature values. The discussions focus on four key performance metrics: output power, efficiency, tracking time, and transient response of the controllers. The results offer valuable insights into the strengths and limitations of each controller, as well as how various optimization algorithms enhance the performance of artificial neural networks.

4.1. Performance of MPPT Controllers in Maximizing PV Output Power

The performance of the proposed hybrid WOVE-NSJ-LM MPPT controller, in terms of PV output power extracted and efficiency, is compared with other benchmark controllers in Figure 7 and Figure 8. The results presented are the maximum steady-state PV output power and efficiency under a fixed irradiance of 1000 W/m², while varying ambient temperatures at 30°C, 25°C, and 20°C. The efficiency corresponding to each temperature value is computed using (6), where the steady state maximum power is taken as a percentage of the theoretical maximum power of 5875 W at 30°C, 6004 W at 25°C, and 6133 W at 20°C.

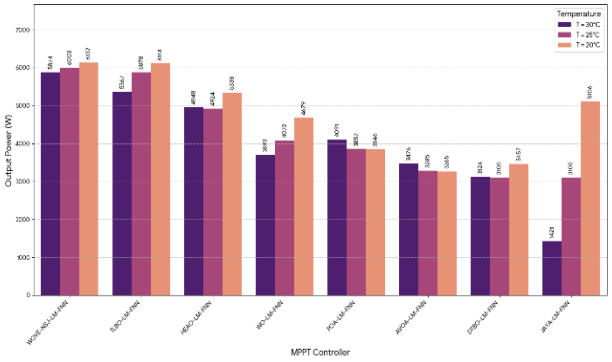

Figure 7. Comparison of steady-state output power across different temperatures and constant irradiance

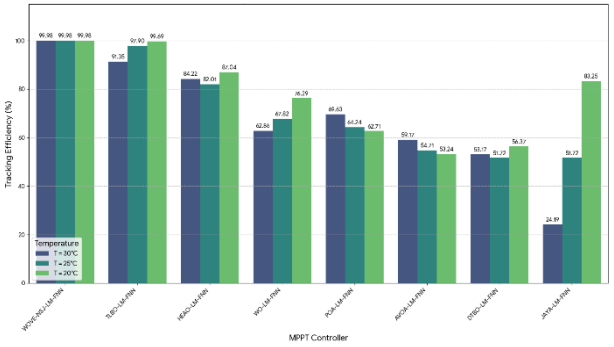

Figure 8. Comparison of tracking efficiency across different temperatures and constant irradiance

At 30°C, the proposed WOVE-NSJ-LM MPPT controller demonstrated outstanding performance, producing a maximum output power of 5,874 W and an efficiency of 99.98%. The efficiency value indicates that the WOVE-NSJ-LM training algorithm was effective in determining and fine-tuning the weights and biases of the feedforward neural network (FNN). In comparison, the TLBO-LM-FNN controller produced a maximum output power of 5367 W with an efficiency of 91.35%. These results placed the TLBO-LM-FNN controller second to the WOVE-NSJ-LM-FNN in terms of maximum power produced. The other controllers, HEAO-LM-FNN and WO-LM-FNN, showed moderate performances. However, JAYA-LM-FNN and DTBO-LM-FNN controllers produced suboptimal power outputs of 1421 W and 3124 W, respectively, representing efficiencies of 24.19% and 53.17%. The JAYA-LM-FNN and DTBO-

LM-FNN controllers were unable to address the temperature-induced variations in PV characteristics effectively. As we lowered the temperature to 25°C, the WOVE-NSJ-LM-FNN controller produced a maximum output power of 6,003 W, representing an efficiency of 99.98%.

The TLBO-LM-FNN controller also performed well, generating an output power of 5878 W with an efficiency of 97.90%. The HEAO-LM-FNN ranked third, with a maximum power output of 4924 W and an efficiency of 82.01%. In contrast, the JAYA-LM-FNN controller demonstrated a significant improvement over its performance at 30°C, with an output power of 3105 W and an efficiency of 51.72%. Meanwhile, POA-LM-FNN and AVOA-LM-FNN exhibited an average performance, while the WO-LM-FNN showed a slight increase in efficiency compared to its output at 30°C. Again, when the temperature was dropped to 20°C, the performance trends among the various artificial neural network (FNN) controllers remained consistent with those at 30°C and 25°C. The WOVE-NSJ-LM-FNN controller demonstrated superior performance, producing an output power of 6,132 W with an efficiency of 99.98%.

The TLBO-LM-FNN controller remained competitive, producing a slightly lower output power of 6,114 W, which represents an efficiency of 99.69%. In contrast, the HEAO-LM-FNN controller produced an output power of 5,338 W, representing an efficiency of 87.04%. Notably, the JAYA-LM-FNN controller, which previously exhibited suboptimal performance, showed some improvement with a power output of 5,106 W, representing an efficiency of 83.25%. The JAYA-LM-FNN controller showed an enhanced adaptability under reduced thermal stress. Conversely, the POA-LM-FNN, AVOA-LM-FNN, and DTBO-LM-FNN controllers still underperformed relative to the WOVE-NSJ-LM-FNN and TLBO-LM-FNN controllers. The consistent and accurate performance of the WOVE-NSJ-LM-FNN controller across all temperature scenarios indicates that the proposed controller performs well under the tested temperature conditions. The WOVE-NSJ-LM-FNN controller's performance can be further attributed to the optimized initial weight and bias selection by the WOVE-NSJ algorithm, which the LM further refines to achieve near-optimal convergence. Additionally, the TLBO-LM-FNN controller was a strong contender, with its performance closely matching that of the WOVE-NSJ-LM-FNN model at lower temperatures. However, the WOVE-NSJ-LM-FNN controller's performance was slightly higher than the TLBO-LM-FNN controller. The consistent and accurate performance of the WOVE-NSJ-LM-FNN controller across all temperature scenarios indicates that the proposed controller performs well under the tested temperature conditions.

On the other hand, JAYA-LM-FNN controller's significant improvement at lower temperatures indicates that it has the potential to perform under certain viable conditions. Finally, the moderate performance of the HEAO-LM-FNN controller, particularly at higher temperatures, and the consistent underperformance of AVOA-LM-FNN, POA-LM-FNN, and DTBO-LM-FNN controllers show their relative inefficiency in extracting maximum power from the PV system.

4.2. Evaluation of Average Power Extraction for FNN-Based MPPT Controllers Under Varying Temperature and Constant Irradiance

In Figure 9**,** the average output power of the various FNN-based MPPT controllers across the three temperature conditions simulated: 30°C, 25°C, and 20°C, already discussed, was computed, and compared. The results in the figure represents the average power extracted across a constant irradiance of 1000 W and varying temperatures of 30°C, 25°C, and 20°C.

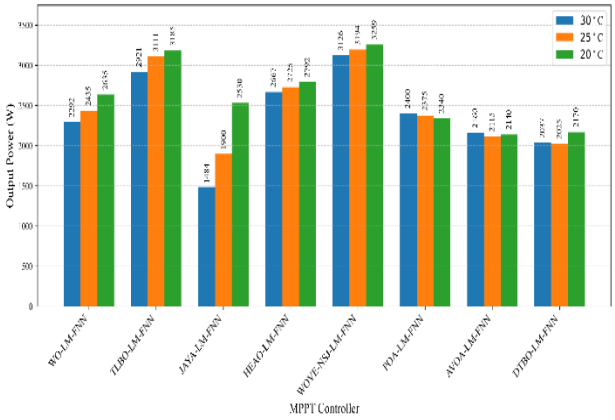

Figure 9. PV Average Output Power at Constant Irradiance (1000 W/m^2)

The WOVE-NSJ-LM-FNN MPPT controller produced the highest average power across all temperatures, with values of 3125.67 W, 3194.00 W, and 3259.00 W at 30°C, 25°C, and 20°C, respectively. The TLBO-LM-FNN controller ranked second in performance with a high average power extraction across all temperatures. For instance, at 25°C, the TLBO-LM-FNN Controller produced 3111.00 W compared to 3194.00 W by the WOVE-NSJ-LM-FNN MPPT controller. The other MPPT controllers showed an expected increase in output power as the temperature was decreased. These results are consistent with the known temperature dependence of PV modules, where lower temperatures improve panel

efficiency. For example, the WO-LM-FNN controller exhibited a significant increase in power, from 2292.00 W at 30°C to 2635.00 W at 20°C. The HEAO-LM-FNN controller also reflected this trend, with a power increase from 2667.00 W to 2792.33 W over the same temperature range.

However, POA-LM-FNN and AVOA-LM-FNN controllers deviated from this trend. These MPPT controllers exhibited less pronounced and inverse variations in output power, indicating that these controllers may have a potential difficulty in adapting to temperature-induced changes in PV module characteristics. Also, JAYA-LM-FNN and DTBO-LM-FNN controllers exhibited relatively lower performance compared to other controllers. At 30°C, the JAYA-LM-FNN controller produced 1483.67 W, which was significantly lower than that of the WOVE-NSJ-LM-FNN and TLBO-LM-FNN controllers. Similarly, the DTBO-LM-FNN controller produced an average output power of 2037.00 W at the same temperature. Finally, the AVOA-LM-FNN controller also underperformed, as its output power produced was relatively low. For instance, at 25°C, the AVOA-LM-FNN controller produced an average output power of 2114.67 W.

As discussed in the results, the WOVE-NSJ-LM-FNN and TLBO-LM-FNN controllers exhibited robust performance due to their high average output power and consistent trends across different simulated temperatures.

4.3. Evaluation of Efficiency Under Random Irradiances

The performance of the various ANN-based MPPT controllers under varying irradiance levels of 1000 W/m², 500 W/m², and 100 W/m², as well as at a standard temperature of 25°C, was also assessed. The results obtained are compared in Figure 10.

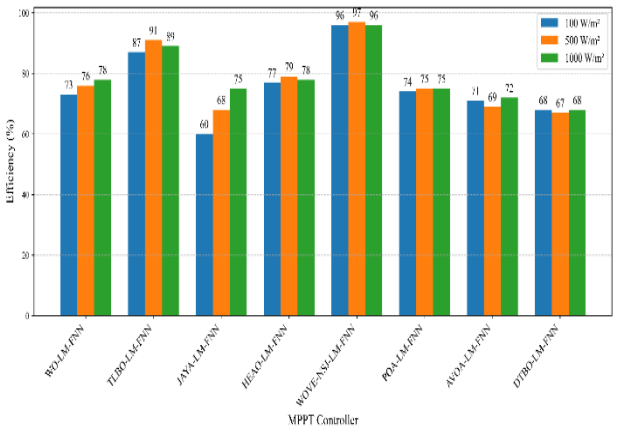

Figure 10. Efficiency of ANN-Based Controllers at Different Irradiances

The WOVE-NSJ-LM-FNN controller had the highest efficiency across all irradiance levels with values of 96%, 97%, and 96% at 100 W/m², 500 W/m², and 1000 W/m², respectively. The TLBO-LM-FNN controller followed closely as the second-best efficient controller, with a maximum efficiency of 91% at 500 W/m² and a minimum efficiency of 87% at 100 W/m². The other controllers, such as WO-LM-FNN, HEAO-LM-FNN, and POA-LM-FNN, exhibited efficiencies in the range of 73–79% with stable performance across different levels. On the other hand, JAYA-LM-FNN, AVOA-LM-FNN, and DTBO-LM-FNN consistently underperformed, with efficiencies ranging from 60% to 75%. The JAYA-LM-FNN controller, however, improved significantly with an efficiency of 75% at 1000 W/m². Clearly, the proposed WOVE-NSJ-LM-FNN controller was robust and efficient in the tracking at different irradiance levels.

4.4. Tracking Time Analysis of FNN-Based MPPT Controllers at Standard Conditions

In Table 5, we compare the tracking time of the MPPT controllers under standard temperature of 25°C and varying irradiance levels.

Table 5. Comparison of average tracking time across varying irradiances of 1000 W/m^2, 750 W/m^2, 500 W/m^2, 250 W/m^2 and 100 W/m^2

MPPT Controller	Tracking time in seconds at varying irradiances				
	100 W/m²	250 W/m²	500 W/m²	750 W/m²	1000 W/m²
WO-LM-FNN	0.319	0.103	0.054	0.5	0.04
TLBO-LM-FNN	0.391	0.125	0.084	0.064	0.045
JAYA-LM-FNN	0.333	0.207	0.06	0.046	0.03
HEAO-LM-FNN	0.219	0.102	0.066	0.052	0.049
WOVE-NSJ-LM-FNN	0.207	0.09	0.068	0.057	0.035
POA-LM-FNN	0.386	0.111	0.066	0.062	0.043
AVOA-LM-FNN	0.351	0.119	0.076	0.052	0.032
DTBO-LM-FNN	0.322	0.136	0.079	0.055	0.041

According to the results in the table, the proposed WOVE-NSJ-LM-FNN consistently had the shortest tracking times, ranging from 0.207 seconds at 100 W/m² to 0.035 seconds at 1000 W/m². The HEAO-LM-FNN controller also demonstrated stable performance with relatively low tracking times across all irradiances. The AVOA-LM-FNN controller also had shorter tracking time under high irradiance but lagged slightly at lower

levels. In contrast, the JAYA-LM-FNN controller also demonstrated excellent and minimal tracking speed at high irradiance levels but struggled significantly at lower irradiance levels. The TLBO-LM-FNN and DTBO-LM-FNN performed more slowly overall in terms of tracking performance. The classical WO-LM-FNN and POA-LM-FNN controllers exhibited noticeable delays under low irradiance levels. Collectively, these results demonstrate that the proposed WOVE-NSJ-LM-FNN controller is efficient in extracting maximum power at lower tracking times. The average tracking times of all controllers are compared in Figure 11.

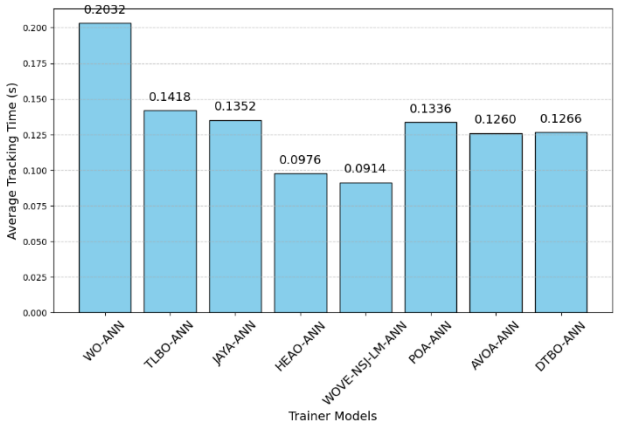

Figure 11. Comparison of average tracking times of ANN-based MPPT controllers under different irradiance and standard temperature of 25°C

The average tracking time of the proposed WOVE-NSJ-LM-FNN was the shortest at 0.0914 seconds. The HEAO-LM-FNN controller closely followed with an average tracking time of 0.0976 seconds. The POA-LM-FNN, AVOA-LM-FNN, and DTBO-LM-FNN had average tracking times of 0.1336 seconds, 0.1260 seconds, and 0.1266 seconds, respectively. The JAYA-LM-FNN and TLBO-LM-FNN controllers had average tracking times of 0.1352 seconds and 0.1418 seconds, respectively, which are relatively higher. However, the average tracking time of the WO-LM-FNN controller was the highest at 0.2032 seconds.

4.5. Transient Power Response Analysis of FNN-Based MPPT Controllers

In Figure 12, we simulated transient scenarios using varying temperatures and irradiance levels and compared the power change responses of the various controllers. The conditions used for simulating the transient scenarios are T = 30°C, I = 1000W/m^2 (first scenario), T = 25°C, I = 750W/m^2 (second scenario), and T = 18°C, I = 500 W/ m^2 (third scenario).

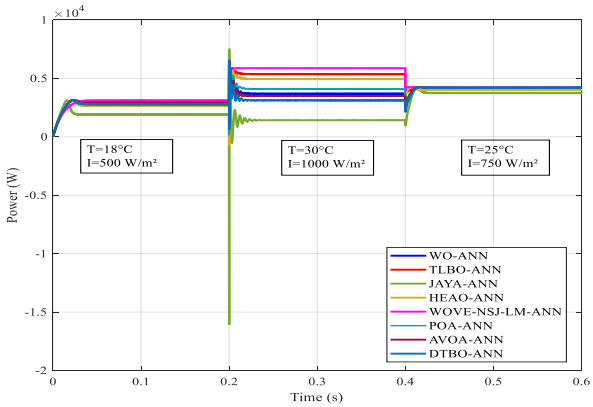

Figure 12. Comparison of the power transient response of controllers to scenario simulation

In a well-designed solar tracking system, overshoot is a key factor to minimize because excessive deviation from the optimal power point wastes energy and can lead to instability. The percentage overshoot of each algorithm is compared to the proposed WOVE-NSJ-LM-FNN in Table 6.

Table 6. Comparison of the percentage overshoot for the power response

Training Algorithm	Percentage Overshoot for different time periods on the transient curve		
	(0 - 0.2) s	(0.2 - 0.4) s	(0.4 - 0.6) s
AVOA-LM-FNN	9.87910	37.28400	1.43060
DTBO-LM-FNN	11.53400	48.76500	1.42970
HEOA-LM-FNN	16.84900	10.60000	5.17580
JAYA-LM-FNN	58.05000	126.47000	11.95800
POA-LM-FNN	13.25200	22.50600	0.00002
TLBO-LM-FNN	6.78860	5.33080	0.00029
WO-LM-FNN	9.87910	31.72000	0.11396
WOVE-NSJ-LM-FNN	0.00002	0.00575	0.00342

As compared in Table 6, WOVE-NSJ-LM-FNN achieved virtually zero overshoot across all observed time intervals: 0.00002% (0–0.2 s), 0.00575% (0.2–0.4 s), and 0.00342% (0.4–0.6 s). These results show the MPPT's exceptional transient stability and precise convergence to the steady-state operating point. The integration of WOVE-NSJ and LM mechanisms in a hybrid MPPT controller resulted in highly effective weight initialisation and adaptive learning dynamics for the FNN.

On the other hand, the JAYA-LM MPPT demonstrated severe instability, with overshoot values reaching 58.05% in the initial interval and peaking at an excessive 126.47% between 0.2 and 0.4 seconds, before dropping to 11.95% in the final phase. Overshoots exceeding 100% are unacceptable in MPPT systems, as they not only reflect poor control performance but also pose risks of hardware stress and energy loss. The JAYA-LM

MPPT lacked the damping characteristics necessary for smooth transient response. Moderate overshoot levels were observed in AVOA-LM (37.28%), DTBO-LM (48.76%), WO-LM (31.72%), and POA-LM (22.51%) during the 0.2–0.4 s interval. Although these values are significantly lower than those of JAYA-LM, they still exceed the thresholds typically considered acceptable for MPPT operation. Among the other MPPT controllers, TLBO-LM emerged as the most stable alternative to WOVE-NSJ-LM. It maintained overshoot below 6.79% in the first interval and exhibited controlled behaviour throughout the remaining time periods. Overall, the comparative analysis shows WOVE-NSJ-LM as the best-performing MPPT algorithm among those tested in terms of transient response and control stability.

Again, the settling times of each MPPT controller are compared in Table 7 during the same time periods.

Table 7. Comparison of settling time for power response

Training Algorithm	Settling time for different time periods on the transient curve		
	(0 - 0.2) s	(0.2 - 0.4) s	(0.4 - 0.6) s
AVOA-LM-FNN	3.20E-02	1.55E-02	1.02E-02
DTBO-LM-FNN	3.15E-02	1.55E-02	1.12E-02
HEOA-LM-FNN	3.02E-02	1.35E-02	1.28E-02
JAYA-LM-FNN	2.52E-02	1.87E-02	2.05E-02
POA-LM-FNN	3.11E-02	1.51E-02	1.38E-02
TLBO-LM-FNN	3.30E-02	1.01E-02	7.94E-03
WO-LM-FNN	3.20E-02	1.54E-02	1.31E-02
WOVE-NSJ-LM-FNN	3.31E-02	4.50E-05	0.00E+00

The settling time analysis further demonstrates the strong performance of the WOVE-NSJ-LM algorithm in MPPT control. While most algorithms achieved settling times within the 10–30 ms range, WOVE-NSJ-LM demonstrated an almost instantaneous response, reaching the steady-state maximum power point in just 4.5×10^{-5} s during the 0.2–0.4 s interval and achieving a complete settling time of 0.00 s by 0.4–0.6 s. This performance indicates that the controller eliminates overshoot and converges to the optimal operating point with faster speed. TLBO-LM exhibited the next best performance among the remaining algorithms, with a fast-settling time of 7.94 ms in the final interval. However, it still fell short of the near-instantaneous response of WOVE-NSJ-LM. Other algorithms, including WO-LM, POA-LM, HEOA-LM, AVOA-LM, DTBO-LM, and JAYA-LM, recorded longer settling times ranging from 10 to 30 ms. Notably, JAYA-LM again underperformed, with a final settling time of 20.5 ms. These findings demonstrate the effectiveness of combining WOVE-NSJ global weight initialization with Levenberg–Marquardt fine-tuning. The proposed hybrid MPPT controller produced negligible overshoot and a near-instantaneous settling time, with high responsiveness to rapid changes in irradiance and temperature.

4.6. Transient Voltage Response Analysis of FNN-Based MPPT Controllers

In Figure 13, voltage transient scenarios are simulated using varying temperatures and irradiance levels. The conditions simulated are T = 30°C, I = 1000W/m^2 (first scenario), T = 25°C, I = 750W/m2 (second scenario), and T = 18°C, I = 500 W/ m^2 (third scenario).

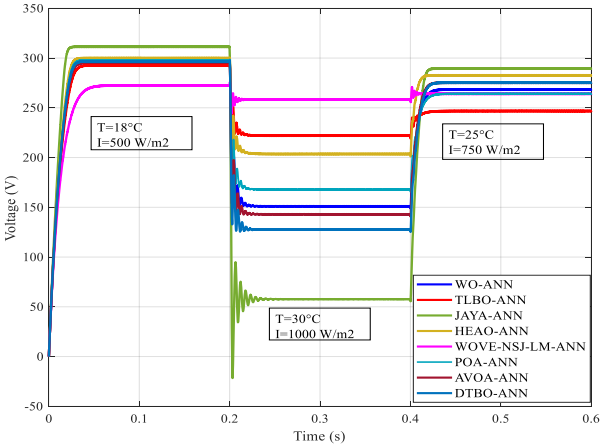

Figure 13. Comparison of the voltage transient response of controllers to scenario simulations

The settling time of each MPPT controller for the voltage transient is compared in **Table 8** for the same time intervals.

Table 8. Comparison of settling time for voltage response

Training Algorithm	Settling time for different time periods on the transient curve		
	0 - 0.2	0.2 - 0.4	0.4 - 0.6
AVOA-LM	2.81E-02	1.55E-02	1.78E-02
DTBO-LM	2.74E-02	1.55E-02	1.88E-02
HEOA-LM	2.58E-02	1.37E-02	1.09E-02
JAYA-LM	2.05E-02	1.87E-02	1.75E-02
POA-LM	2.68E-02	1.51E-02	1.88E-02
TLBO-LM	2.96E-02	1.04E-02	9.17E-03
WO-LM	2.81E-02	1.54E-02	1.92E-02
WOVE-NSJ-LM	3.96E-02	0.00E+00	0.00E+00

In terms of voltage response, most algorithms settled within the expected range of 10–30 ms. Notably, WOVE-NSJ-LM showed a distinct advantage by achieving a settling time of 0.00 s in both the 0.2–0.4 s and 0.4–0.6 s intervals, indicating an immediate transition to steady-state without delay. TLBO-LM and HEOA-LM also performed well, with settling times of 9.17 ms and 10.9 ms, respectively, in the final interval. These values exhibit rapid stabilization, although not as rapidly as those of WOVE-NSJ-LM. JAYA-LM recorded moderate settling times, but its earlier overshoot issues limit its overall effectiveness. Overall, the results show that WOVE-NSJ-LM combines fast settling with low overshoot, which is beneficial for maintaining stable voltage in MPPT systems. While other algorithms offer acceptable performance, WOVE-NSJ-LM demonstrates strong performance under the tested transient conditions.

V. Conclusion

The increasing penetration of photovoltaic (PV) systems into modern power networks highlights the importance of reliable and efficient maximum power point tracking (MPPT) to ensure stable power delivery under dynamic environmental conditions. Conventional MPPT methods, such as the Perturb and Observe (P&O) method or classical heuristic controllers, often struggle with slow convergence, entrapment in local optima, poor adaptability to fluctuating irradiance and temperature, and oscillatory steady-state behaviour. These limitations translate into significant power losses and reduced system efficiency. Addressing these challenges formed the core motivation for this research.

To overcome the above limitations, this study proposes a novel hybrid MPPT controller based on the improved Walrus Optimization with Vigilante Selection and Juvenile Update (WOVE-NSJ), combined with the Levenberg–Marquardt (LM) algorithm for training a feedforward neural network (FNN). The WOVE-NSJ algorithm was designed to enhance the balance between exploration and exploitation during the weight initialization of the FNN, thereby avoiding premature convergence. The LM algorithm, on the other hand, refines the initialized weights to accelerate convergence and minimize training errors. Together, the hybrid WOVE-NSJ-LM training framework provided an effective tool to address the shortcomings of both conventional MPPT methods and previously explored metaheuristic ANN models.

The proposed WOVE-NSJ-LM-FNN MPPT controller was evaluated against other ANN-based MPPT controllers under varying irradiance and temperature conditions. The results established several key findings:

a) The WOVE-NSJ-LM-FNN consistently achieved near-perfect efficiencies of approximately 99.98% across variations in irradiance and temperature. It outperformed all benchmark controllers, with TLBO-LM-FNN emerging as the closest competitor (up to 97.9%). Controllers such as JAYA-LM-FNN and DTBO-LM-FNN significantly underperformed, particularly at higher temperatures.

b) The proposed controller delivered the highest average power across all tested temperatures, demonstrating superior robustness to thermal variations. TLBO-LM-FNN again ranked second, while POA-LM-FNN and AVOA-LM-FNN failed to adapt effectively to temperature changes.

c) The WOVE-NSJ-LM-FNN exhibited the shortest average tracking time (0.0914 s), significantly outperforming classical WO-LM-FNN (0.2032 s). This demonstrated the proposed controller's ability to achieve rapid convergence to the MPP, which is essential under fluctuating irradiance conditions.

d) In dynamic simulations, WOVE-NSJ-LM-FNN achieved virtually zero overshoot and near-instantaneous settling times (as low as 4.5×10^{-5} s), reflecting exceptional stability and adaptability. By comparison, controllers such as JAYA-LM-FNN exhibited severe instability with overshoot exceeding 100%, while TLBO-LM-FNN maintained moderate but acceptable stability.

e) Voltage transient analysis confirmed that WOVE-NSJ-LM-FNN not only eliminated overshoot but also reached steady-state voltage faster than all other controllers, ensuring both power quality and reliability.

While the proposed controller shows significant promise in simulation studies, future work should extend this research in several directions. First, hardware-in-the-loop (HIL) or real-time experimental validation is needed to verify performance under practical operating conditions. Second, scalability to larger PV arrays and grid-connected systems should be explored, particularly under partial shading scenarios where the complexity of MPPTs increases. Finally, the adaptability of the proposed method to hybrid renewable energy systems (PV–wind, PV–battery) could be investigated to extend its application beyond standalone PV systems.

Declaration

- The authors declare that they have no known financial or non-financial competing interests in any material discussed in this paper.
- The authors declare that this article has not been published before and is not in the process of being published in any other journal.
- The authors confirmed that the paper was free of plagiarism

References

[1] "Renewable energy – powering a safer future | United Nations." Accessed: Oct. 01, 2025. https://www.un.org/en/climatechange/raising-ambition/renewable-energy

[2] "Photovoltaic cells | Research Starters | EBSCO Research." Accessed: Sep. 01, 2025. https://www.ebsco.com/research-starters/environmental-sciences/photovoltaic-cells

[3] M. Tawalbeh, A. Al-Othman, F. Kafiah, E. Abdelsalam, F. Almomani, and M. Alkasrawi, "Environmental impacts of solar photovoltaic systems: A critical review of recent progress and future outlook," Science of The Total Environment, vol. 759, p. 143528, Mar. 2021, doi: 10.1016/j.scitotenv.2020.143528.

[4] G. Masson, M. de l'Epine, and I. Kaizuka, "Trends in PV Applications 2024," Oct. 2024, doi: 10.69766/JNEW6916.

[5] A. El Hammoumi, S. Chtita, S. Motahhir, and A. El Ghzizal, "Solar PV energy: From material to use, and the most commonly used techniques to maximize the power output of PV systems: A focus on solar trackers and floating solar panels," Energy Reports, vol. 8, pp. 11992–12010, Nov. 2022, doi: 10.1016/j.egyr.2022.09.054.

[6] M. E. B. Ghribi, L. Garcia-Gutierrez, Z. E. T. Ternifi, Z. Zheng, G. Bachir, and M. Aillerie, "Tracking the maximum power point of solar panels through direct estimation of optimum voltage with temperature," Clean Energy, vol. 8, no. 4, pp. 135–146, Aug. 2024, doi: 10.1093/ce/zkae044.

[7] H. Chen, L. Xiang, L. Lin, and S. Huang, "Fractional-order PID Load Frequency Control for Power Systems Incorporating Thermostatically Controlled Loads," in Proceedings of 2021 IEEE 4th International Electrical and Energy Conference, CIEEC 2021, Institute of Electrical and Electronics Engineers Inc., May 2021. doi: 10.1109/CIEEC50170.2021.9510621.

[8] A. I. M. Ali and H. R. A. Mohamed, "Improved P&O MPPT algorithm with efficient open-circuit voltage estimation for two-stage grid-integrated PV system under realistic solar radiation," International Journal of Electrical Power & Energy Systems, vol. 137, p. 107805, May 2022, doi: 10.1016/j.ijepes.2021.107805.

[9] K. S. Tey and S. Mekhilef, "Modified incremental conductance MPPT algorithm to mitigate inaccurate responses under fast-changing solar irradiation level," Solar Energy, vol. 101, pp. 333–342, Mar. 2014, doi: 10.1016/j.solener.2014.01.003.

[10] J. Ahmad, "A fractional open circuit voltage based maximum power point tracker for photovoltaic arrays," in 2010 2nd International Conference on Software Technology and Engineering, IEEE, Oct. 2010. doi: 10.1109/ICSTE.2010.5608868.

[11] N. F. Ibrahim et al., "A new adaptive MPPT technique using an improved INC algorithm supported by fuzzy self-tuning controller for a grid-linked photovoltaic system," PLoS One, vol. 18, no. 11, p. e0293613, Nov. 2023, doi: 10.1371/journal.pone.0293613.

[12] J. T. Sousa and R. S. Barbosa, "Comparison of Classical and Artificial Intelligence Algorithms to the Optimization of Photovoltaic Panels Using MPPT," Algorithms, vol. 18, no. 8, p. 493, Aug. 2025, doi: 10.3390/a18080493.

[13] D. Devikanniga, K. Vetrivel, and N. Badrinath, "Review of meta-heuristic optimization based artificial neural networks and its applications," J Phys Conf Ser, vol. 1362, no. 1, 2019, doi: 10.1088/1742-6596/1362/1/012074.

[14] M. Han, Z. Du, K. F. Yuen, H. Zhu, Y. Li, and Q. Yuan, "Walrus optimizer: A novel nature-inspired metaheuristic algorithm," Expert Syst Appl, vol. 239, p. 122413, Apr. 2024, doi: 10.1016/j.eswa.2023.122413.

[15] A. Saberi, M. Niroomand, and B. M. Dehkordi, "An Improved P&O Based MPPT for PV Systems with Reduced Steady-State Oscillation," Int J Energy Res, vol. 2023, pp. 1–15, Jul. 2023, doi: 10.1155/2023/4694583.

[16] M. Nkambule, A. Hasan, and A. Ali, "Proportional study of Perturb & Observe and Fuzzy Logic Control MPPT Algorithm for a PV system under different weather conditions," in 2019 IEEE 10th GCC Conference & Exhibition (GCC), IEEE, Apr. 2019, pp. 1–6. doi: 10.1109/GCC45510.2019.1570516142.

[17] J. López Seguel, S. I. Seleme Jr, and L. M. F. Moráis, "Comparison of the performance of MPPT methods applied in converters Buck and Buck-Boost for autonomous photovoltaic systems," Ingeniare. Revista chilena de ingeniería, vol. 29, no. 2, pp. 229–244, Jun. 2021, doi: 10.4067/S0718-33052021000200229.

[18] H. A. Sher, A. F. Murtaza, A. Noman, K. E. Addoweesh, and M. Chiaberge, "An intelligent control strategy of fractional short circuit current maximum power point tracking technique for photovoltaic applications," Journal of Renewable and Sustainable Energy, vol. 7, no. 1, Jan. 2015, doi: 10.1063/1.4906982.

[19] D. Baimel, S. Tapuchi, Y. Levron, and J. Belikov, "Improved Fractional Open Circuit Voltage MPPT Methods for PV Systems," Electronics (Basel), vol. 8, no. 3, p. 321, Mar. 2019, doi: 10.3390/electronics8030321.

[20] A. Hassan, O. Bass, and M. A. S. Masoum, "An improved genetic algorithm based fractional open circuit voltage MPPT for solar PV systems," Energy Reports, vol. 9, pp. 1535–1548, Dec. 2023, doi: 10.1016/j.egyr.2022.12.088.

[21] M. Z.-E. Masry, A. Mohammed, F. Amer, and R. Mubarak, "New Hybrid MPPT Technique Including Artificial Intelligence and Traditional Techniques for Extracting the Global Maximum Power from Partially Shaded PV Systems," Sustainability, vol. 15, no. 14, p. 10884, Jul. 2023, doi: 10.3390/su151410884.

[22] Q. Pang, F. Zhang, S. Han, T. Zhou, and Y. Wang, "A new two-stage MPPT technique for enhancing the performance of PV system," Electrical Engineering, vol. 107, no. 8, pp. 10899–10909, Aug. 2025, doi: 10.1007/s00202-025-03067-x.

[23] I. S. Millah, P. C. Chang, D. F. Teshome, R. K. Subroto, K. L. Lian, and J.-F. Lin, "An Enhanced Grey Wolf Optimization Algorithm for Photovoltaic Maximum Power Point Tracking Control Under Partial Shading Conditions," IEEE Open Journal of the Industrial Electronics Society, vol. 3, pp. 392–408, 2022, doi: 10.1109/OJIES.2022.3179284.

[24] M. E. Başoğlu, "A Fast GMPPT Algorithm Based on PV Characteristic for Partial Shading Conditions," Electronics (Basel), vol. 8, no. 10, p. 1142, Oct. 2019, doi: 10.3390/electronics8101142.

[25] B. Mbarki, F. Fethi, J. Chrouta, and A. Zaafouri, "Adaptive neuro-fuzzy inference system algorithm-based robust terminal sliding mode control MPPT for a photovoltaic system," Transactions of the Institute of Measurement and Control, vol. 46, no. 2, pp. 316–325, Jan. 2024, doi: 10.1177/01423312231173022.

[26] B. C. Phan, Y.-C. Lai, and C. E. Lin, "A Deep Reinforcement Learning-Based MPPT Control for PV Systems under Partial Shading Condition," Sensors, vol. 20, no. 11, p. 3039, May 2020, doi: 10.3390/s20113039.

[27] S. S. Saad, M. A. Atiqi Mohd Zainuri, and A. Hussain, "Implementation of Maximum Power Point Tracking Techniques for PV-Wind Hybrid Energy System: A Review," in 2021 International Conference on Electrical Engineering and Informatics (ICEEI), IEEE, Oct. 2021, pp. 1–6. doi: 10.1109/ICEEI52609.2021.9611148.

[28] Y. Li, L. Li, Z. Lian, K. Zhou, and Y. Dai, "A quasi-opposition learning and chaos local search based on walrus optimization for global optimization problems," Sci Rep, vol. 15, no. 1, p. 2881, Jan. 2025, doi: 10.1038/s41598-025-85751-3.

[29] L. Abualigah et al., "An enhanced Walrus Optimizer with opposition-based learning and mutation strategy for data clustering," Array, vol. 26, p. 100409, Jul. 2025, doi: 10.1016/j.array.2025.100409.

[30] P. Trojovský and M. Dehghani, "Walrus Optimization Algorithm: A New Bio-Inspired Metaheuristic Algorithm," Oct. 24, 2022. doi: 10.21203/rs.3.rs-2174098/v1.

[31] P. Rajarajeswari, B. D. V, and A. L. M. S, "Hybrid Termite Queen and Walrus Optimization Algorithm-based energy efficient cluster-based routing with static and mobile sink node in WSNs," Peer Peer Netw Appl, vol. 18, no. 2, p. 8, Mar. 2025, doi: 10.1007/s12083-024-01848-y.

[32] S. Vujošević, M. Ćalasan, and M. Micev, "Hybrid walrus optimization algorithm techniques for optimized parameter estimation in single, double, and triple diode solar cell models," AIP Adv, vol. 14, no. 8, Aug. 2024, doi: 10.1063/5.0223492.

[33] J. He, Y. Tang, X. Guo, H. Chen, and W. Guo, "Research on hybrid reservoir scheduling optimization based on improved walrus optimization algorithm with coupling adaptive ε constraint and multi-strategy optimization," Sci Rep, vol. 14, no. 1, p. 11981, May 2024, doi: 10.1038/s41598-024-62722-8.

[34] Y. Ke, L. Shi, W. Ji, P. Luo, and L. Guo, "Application of the Multi-Strategy Improved Walrus Optimization Algorithm in Mobile Robot Path Planning," IEEE Access, vol. 12, pp. 184216–184229, 2024, doi: 10.1109/ACCESS.2024.3506977.

[35] S. Lv, J. Zhuang, Z. Li, H. Zhang, H. Jin, and S. Lü, "An enhanced walrus optimization algorithm for flexible job shop scheduling with parallel batch processing operation," Sci Rep, vol. 15, no. 1, p. 5699, Feb. 2025, doi: 10.1038/s41598-025-89527-7.

[36] Y. Geng, Y. Li, and C. Deng, "An Improved Binary Walrus Optimizer with Golden Sine Disturbance and Population Regeneration Mechanism to Solve Feature Selection Problems," Biomimetics, vol. 9, no. 8, p. 501, Aug. 2024, doi: 10.3390/biomimetics9080501.

[37] H. M. Hasanien, I. Alsaleh, Z. Ullah, and A. Alassaf, "Probabilistic optimal power flow in power systems with Renewable energy integration using Enhanced walrus optimization algorithm," Ain Shams Engineering Journal, vol. 15, no. 3, p. 102663, Mar. 2024, doi: 10.1016/j.asej.2024.102663.

[38] A. Dev et al., "Improved Extraction of Parameters of Solar PV Cell Diode Model Using Marine Walrus Inspired Optimization Algorithm," IEEE Access, vol. 12, pp. 181217–181231, 2024, doi: 10.1109/ACCESS.2024.3504559.

[39] S. E. V. S. Pillai, G. S. Nadella, K. Meduri, N. A. Priyadharsini, A. Bhuvanesh, and D. Kumar, "A walrus optimization-enhanced long short-term memory model for credit fraud detection in banking," International Journal of Information Technology, May 2025, doi: 10.1007/s41870-025-02574-1.

[40] V. K. R. M and A. C, "Secure Clustering and Routing Based Multi Objective Walrus Optimization

Algorithm for Wireless Sensor Networks," International Journal of Electrical and Electronics Engineering, vol. 12, no. 1, pp. 211–221, Jan. 2025, doi: 10.14445/23488379/IJEEE-V12I1P121.

[41] J. Li, R. Lu, B. Zeng, J. Zhang, Y. Deng, and H. Feng, "Multi-threshold medical image segmentation based on the enhanced walrus optimizer," J Supercomput, vol. 81, no. 4, p. 513, Feb. 2025, doi: 10.1007/s11227-025-07023-1.

[42] A. Kumar and R. Agarwal, "Mathematical Modeling and Analysis of Single-Diode, Double-Diode and Triple Diode based PV Module," in 2023 International Conference for Advancement in Technology, ICONAT 2023, Institute of Electrical and Electronics Engineers Inc., 2023. doi: 10.1109/ICONAT57137.2023.10080741.

[43] I. Haseeb et al., "Solar Power System Assessments Using ANN and Hybrid Boost Converter Based MPPT Algorithm," Applied Sciences, vol. 11, no. 23, p. 11332, Nov. 2021, doi: 10.3390/app112311332.

[44] J. Zupan, "Introduction to Artificial Neural Network (ANN) Methods: What They Are and How to Use Them*," 1994.